

A Nanofoaming Process and Dielectric Properties of Polymethylphenylsilsesquioxane-Based Nanofoams

Soo Man Hong, Seung Sang Hwang

Polymer Hybrids Research Center, Korea Institute of Science and Technology, Cheongryang, Seoul 130–650, Korea

Received 16 June 2005; accepted 27 October 2005

DOI 10.1002/app.23809

Published online in Wiley InterScience (www.interscience.wiley.com).

ABSTRACT: We prepared polymethylphenylsilsesquioxane (PMPSQ) as an inorganic, thermally stable, matrix and poly-D,L-lactide-1,6-hexanediol (PDLLA-1,6-hexanediol) as a porogen material. PMPSQ was initially designed to obtain synergistic effects from polyphenylsilsesquioxane and poly-methylsilsesquioxane. The PDLLA-1,6-hexanediol was chosen as a porogen since it has a much lower thermal stability when compared with PMPSQ. The initial decomposition temperature of the PMPSQ (458°C) was higher than the terminal decomposition temperature of PDLLA-1,6-hexanediol by 148°C, resulting in a broad processing window for the nanofoaming process. The broad window was utilized not only for optimization of the foaming condition, but for preparation of the nanofoamed PMPSQ without disruption in the structural stability of the matrix. Furthermore, hydroxyl end groups on PMPSQ and PDLLA-1,6-hexanediol

played a role in the uniform and well-distributed phase separation behavior. PMPSQ and PDLLA-1,6-hexanediol were investigated by ¹H NMR, GPC, and thermogravimetric analysis to characterize the properties of polymers and optimize the foaming condition. The inorganic/organic hybrids based on the PMPSQ and PDLLA-1,6-hexanediol were prepared and measured in terms of phase separation behavior and dielectric properties. In these hybrid systems, PMPSQ/PDLLA-1,6-hexanediol (85/15) exhibited the most uniform and the smallest nanofoam distribution in the continuous PMPSQ matrix. © 2006 Wiley Periodicals, Inc. *J Appl Polym Sci* 100: 4964–4971, 2006

Key words: polymethylphenylsilsesquioxane; poly-D,L-lactide-1,6-hexanediol; dielectric constant; phase separations; nanofoaming

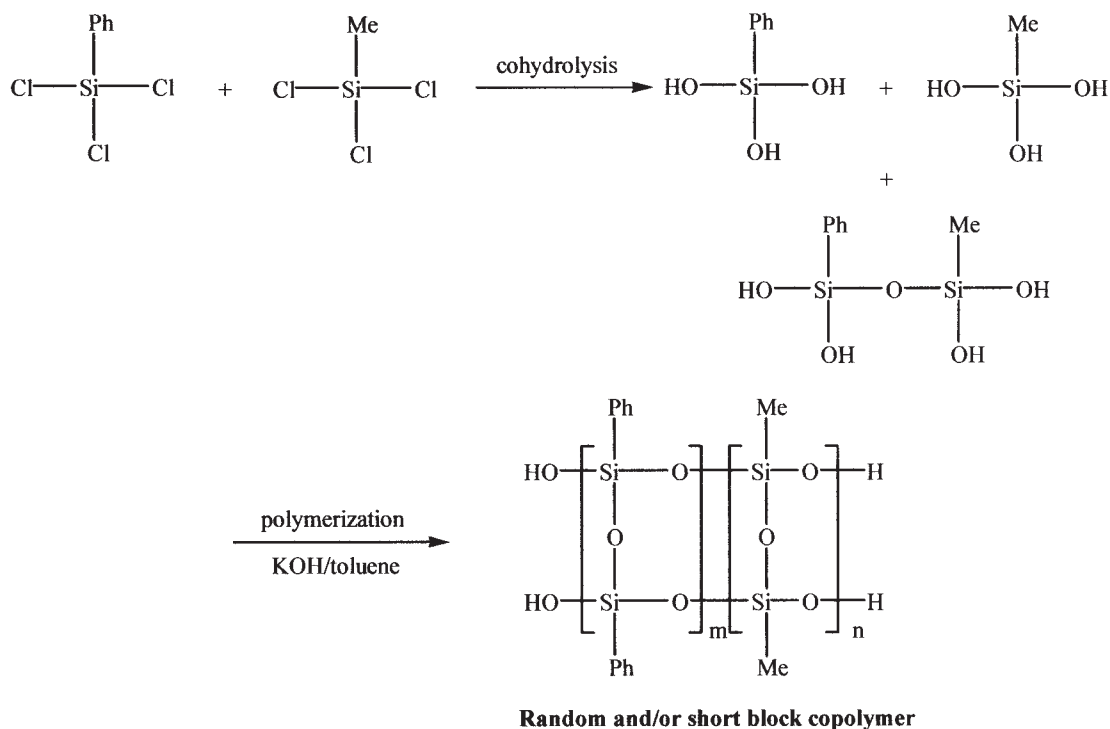
INTRODUCTION

As modern technology requires smaller and faster microelectronic devices, a number of attempts have been made to develop new microelectronic packaging materials.¹ Various types of polyimides are potential candidates as microelectronic insulators and have been actively investigated because of their high thermal stability, good mechanical properties, low thermal expansion coefficients, and comparatively low dielectric constants (~3.2).^{2,3} However, materials with a dielectric constant much lower than 3.0 are needed as the size of logic chips decreases below 0.5 μm to reduce the RC delay and crosstalk problems. One way to prepare such a low K material was to obtain polyimide nanofoams attempted by many research groups at IBM Almaden Research Center.^{4–7} However, polyimides have drawbacks in their application to microelectronic packaging materials because of their anisotropic physical properties, high H₂O pick-up, and foam collapse above 370°C during the nanofoaming process.

Novel candidates such as SiLK,⁸ benzocyclobutene resin,⁹ poly(perfluorocyclobutane),¹⁰ and poly(silsesquioxane)¹¹ for microelectronic application have been investigated. One of the most promising candidates for low K materials is polyorganosilsesquioxane (PSSQ). PSSQs have attracted scientific interest not only because of their low dielectric constants (2.6–2.8), but also because of their excellent thermal stabilities, low moisture pick-up, and low thermal expansion coefficients.¹² However, the dielectric constant of this material is still too high to be applied to advanced logic chips. Incorporation of air foams into PSSQ would be one way to lower the dielectric constants of the polymers. The nanofoaming process of PSSQ has recently been focused on polymethylsilsesquioxane (PMSQ) because of its excellent physical properties such as good dimensional stability and its ability to be applied to various microelectronic packaging industries in terms of cost savings.^{11,13} Even though PMSQ has outstanding physical properties suitable for the application as mentioned earlier, it has shortcomings when compared with polyphenylsilsesquioxane (PPSQ). For example, although a number of reports on the structural regularity of PPSQ have been reported,^{14–17} few have discussed the well-defined chemical structure of PMSQ. It is generally known that the structure control of PPSQ is much easier than that of PMSQ because of side group effect and steric hin-

Correspondence to: S. M. Hong (smhong@kist.re.kr).

Contract grant sponsor: KIST; contract grant number: 2E16972.



Scheme 1 Synthetic route of PMPSQ.

drance leading to regulated backbone structure. However, the brittle nature and poor gap filling ability of PPSQ have interfered with its industrial applications.

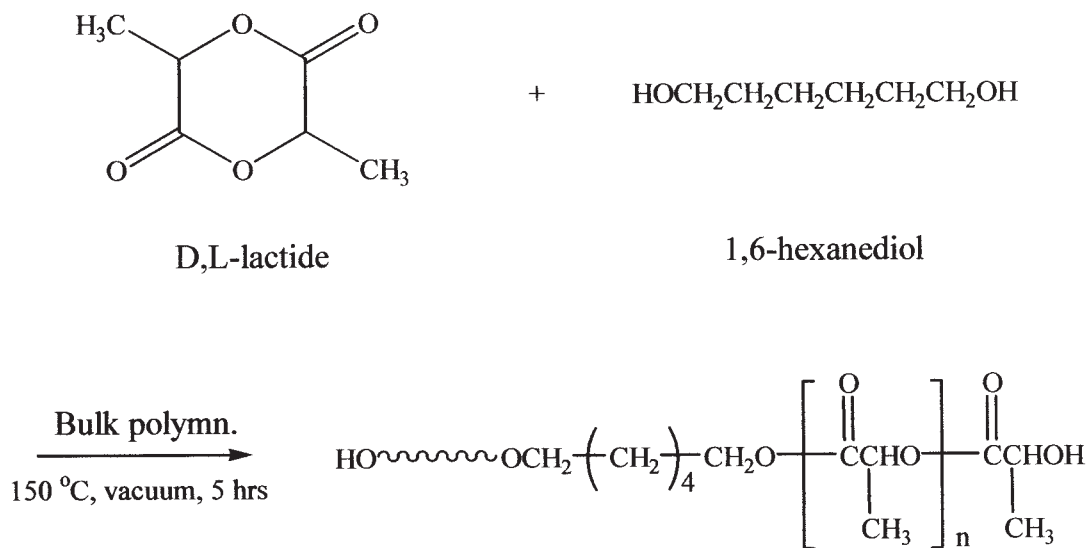
In this study, we prepared polymethylphenylsilsesquioxane (PMPSQ)^{14,18,19} as a matrix and poly-D,L-lactide-1,6-hexanediol (PDLLA-1,6-hexanediol) as a porogen material. PMPSQ was initially designed to obtain the synergistic effects of PPSQ and PMSQ. PDLLA-1,6-hexanediol is an amorphous, flexible, and readily decomposable polymer that has been used in biomaterials such as biodegradable polymers and polymer scaffolds. The amorphous nature of this polymer prevents the crystallization, which causes cracking in the prepared organic/inorganic hybrid films.²⁰ The comparatively long aliphatic block results in a polymer with increased flexibility and enhanced interactions between the methyl groups of PMPSQ and the alkyl groups of PDLLA-1,6-hexanediol through van der Waals forces. Furthermore, hydroxyl end groups on PMPSQ and PDLLA-1,6-hexanediol would also contribute to uniform and well-distributed phase separation behavior. Interestingly, PDLLA-1,6-hexanediol is a thermally labile polymer relative to PMPSQ, resulting in a broad processing window. The broad window for the nanofoaming process would be helpful in obtaining nanofoamed PMPSQ with low dielectric constants. Both the porogen and the matrix are amphiphilic; therefore, high-quality films are expected to be prepared without macroscopic aggregation or precipitation.

EXPERIMENTAL

Preparation of polymers

D,L-lactide (Purac Biochem, Gorinchem, Holland) was purified by recrystallization from dried acetate. It was then dried for 24 h under vacuum prior to use. Potassium hydroxide (KOH) from Sigma-Aldrich was used, without further purification, as a catalyst for preparation of PMPSQ. Stannous octoate (Sn(oct)₂; Sigma, St. Louis, MO) was purified by vacuum distillation at 175°C (~0.2 mmHg). 1,6-Hexanediol of Aldrich was distilled under reduced pressure. Toluene was distilled over sodium metal before use. PMPSQ was synthesized by the method previously described in our papers.¹⁴⁻¹⁹ Mixtures of phenyltrichlorosilane and methyltrichlorosilane with molar ratio of 1/1 were hydrolyzed below 0°C for 3 h. The initial hydrolyzates of the reaction mixture were then dissolved in toluene with a small amount of KOH. The solution was heated up to reflux temperature and stirred for 16 h. The obtained product was then filtered and dried in a vacuum oven at 110°C for 12 h. The yield was 81.78%. The synthetic route of PMPSQ is described in Scheme 1.

PDLLA-1,6-hexanediol was prepared by bulk polymerization. D,L-lactide (17.2 g, 0.119 mol) and 0.598 g (5.00 × 10⁻³ mol) of 1,6-hexanediol were added to a glass ampoule containing a teflon-coated magnetic stirring bar. After 0.269 g (6.60 × 10⁻⁴ mol) of Sn(Oct)₂ was added, the ampoule was sealed under vacuum



Poly(D,L-lactide)-1,6-hexanediol

Scheme 2 Synthetic route of PDLLA-1,6-hexanediol.

after purging thrice with nitrogen at 90°C. The ampoule was heated up to 130°C in an oil bath for 5 h, with stirring. After the reaction was carried out, the ampoule was broken, the product was dissolved in 300 mL of chloroform, and then micro-filtered through a 0.45- μm -pore membrane filter. The polymer solution was evaporated to a final volume of 70 mL. The obtained product was then poured into 700 mL methanol, filtered, and dried under vacuum. The yield of PDLLA-1,6-hexanediol was 86.21%.²¹ Synthetic route of PDLLA-1,6-hexanediol is given in Scheme 2.

¹H NMR (CDCl_3): δ 5.18 (q, 2nH, (OCO(CH)OCO)), 4.38 (q, 2H, (OCO(CH)OH)), 4.17 (t, 4H, ($\text{CH}_2(\text{CH}_2)\text{OCO}$)), 1.59 (d, 6nH, (CH_3)) ppm.

Identification of polymers

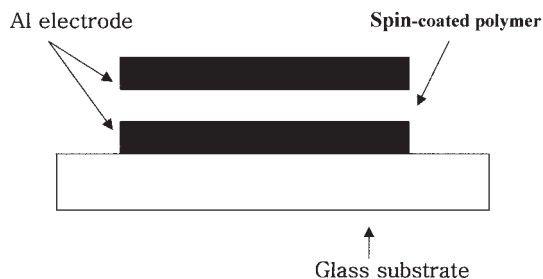
¹H NMR spectra were obtained using a Varian Gemini-200 spectrometer with CDCl_3 as an internal standard. The M_n and molecular weight distribution (MWD) were determined by Waters GPC 410 system. The equipment was composed of five Ultrastaygel[®] columns (10^6 , 2×10^5 , 10^4 , 10^3 g/mol), and the molecular weight was calibrated by polystyrene standards (Polymer Lab.). THF was used as an eluent at a flow rate of 10 mL/min. Thermogravimetric analysis (TGA) was conducted with a TGA 2950 from DuPont instruments Co. Temperature was raised up to 800°C from initial equilibrium temperature of 30°C, at a heating rate of 10°C/min. FT-Raman spectra were recorded on PerkinElmer System 2000 NIR FT-Raman spectrometer equipped with Nd:YAG CW Laser ($\lambda = 1064$ nm) source using the back scattering method.

Specimen preparation and AFM measurement

The PMPSQ and PMPSQ/PDLLA-1,6-hexanediol hybrids at different weight ratios were dissolved in toluene with a concentration of 15% by weight. The compositions of all samples are PMPSQ/PDLLA-1,6-hexanediol hybrid materials of 90/10, 85/15, and 80/20. The solution was spin-coated on a freshly cleaned slide glass after filtering the solution through a Millipore Teflon filter (0.2 μm). The thickness of all the spin-coated films was ~ 1.0 μm . The nanofoamed films were obtained according to the foaming condition described in Figure 3. During AFM measurement, micrographs were recorded with a Multimode Scanning Probe Microscope (Digital Instruments, Inc.). The tapping-mode was used to obtain phase-imaging data with 125- μm -long cantilevers. The cantilever had a very small tip radius of 5–10 nm. The lateral scan frequency was about 1.0 Hz. The sample was moved in the x - y plane and voltage was applied, which moved the piezo driver over the z -axis, to keep the probing force constant, resulting in a three-dimensional height image of the sample surface.

Specimen preparation and measurement of dielectric properties

Aluminum (CERAC[™] specialty inorganics with purity of 99.999%) electrodes were evaporized with a thickness of 1000 Å on a freshly cleaned slide glass by ULVAC VPC-260F vacuum deposition equipment. PMPSQ and PMPSQ/PDLLA-1,6-hexanediol hybrids at different compositions were dissolved in toluene



Scheme 3 The schematic diagram of prepared specimen for measurement of dielectric constants.

with a concentration of 15% by weight. The solution was spin-coated on the aluminum-coated glass after filtering the solution through a Millipore Teflon filter ($0.2\ \mu\text{m}$). All the obtained films were $\sim 1.0\ \mu\text{m}$ thick. The film thickness was measured by P-10 surface profiler from TENCOR Instruments. The films were foamed at the various foaming conditions under nitrogen atmosphere and cooled down to room temperature. Finally, aluminum electrodes were evaporized onto the specimen, resulting in a set of metal-insulator-metal devices (Scheme 3).

Dielectric behavior measurements were carried out on a Hewlett-Packard LF impedance analyzer Model 4192A equipped with a Mettler Toledo FP82HT hot stage and Mettler Toledo FP90 central processor. Temperature was raised up to 100°C from the initial temperature of 30°C . Heating rate was $5^\circ\text{C}/\text{min}$ at a frequency of 1 MHz.

RESULTS AND DISCUSSION

Preparation of polymers

The M_n and MWD of PMPSQ and PDLA-1,6-hexanediol were measured by GPC. The M_n of PMPSQ and PDLA-1,6-hexanediol are 11,430 and 3828, respectively. The MWD of PMPSQ and PDLA-1,6-hexanediol are 1.26 and 1.22, respectively. Other analysis and characterization such as ^1H NMR, ^{29}Si NMR, TGA, and DSC of PMPSQ and PDLA-1,6-hexanediol were reported earlier.^{14,18,19,21}

Optimization of the foaming process

To optimize the foaming conditions for preparation of nanofoamed PMPSQ, the thermal decomposition behaviors of PMPSQ and PDLA-1,6-hexanediol were investigated by TGA, as shown in Figure 1. The initial decomposition temperatures of PMPSQ and PDLA-1,6-hexanediol are 458 and 127°C , respectively. In addition, the terminal decomposition temperature of PDLA-1,6-hexanediol is 310°C . This indicates that the processing window for the nanofoaming process is as large as 148°C . Many researchers have reported on

the nanofoaming process using polyimides and thermally labile organic polymers such as polystyrene and poly(propylene oxide).^{6,7} However, nanofoamed polyimides were not easily obtained because of the cell collapse of the formed air foams in a matrix polymer. The low processing window was one of the reasons. This occurred because the terminal decomposition temperature of the porogen was close enough to induce thermal transition (e.g., T_g) of polyimide.⁷ In the case of silsesquioxanes, an attempt for using nanoporous polymethylsilsesquioxanes (PMSQ) has been investigated.²² However, structural instability of PMSQ during the curing process due to self-aggregation or phase separation of the porogen (nanofoam) phase resulted in large pores ($\sim 400\ \text{nm}$). These large pores can significantly deteriorate mechanical properties of the porous film. This phase separation problem is likely due to early pyrolysis ($\sim 150^\circ\text{C}$) before curing and structural transformation during the curing process of the PMSQ precursor.²³ In contrast, as shown in TGA thermogram data (Fig. 1), PMPSQ used in this study shows no significant difference in terms of thermal stability before and after the curing process. This enhanced thermal and structural stability of PMPSQ also contributes to easier optimization of the foaming condition.

We also checked the thermal decomposition behavior of PMPSQ/PDLA-1,6-hexanediol hybrids using FT-Raman spectroscopy to investigate how the thermally labile polymer (PDLA-1,6-hexanediol) is thermally decomposed. Figure 2 shows FT-Raman spectra of the PMPSQ/PDLA-1,6-hexanediol hybrid material at three different temperatures. Characteristic peaks of Si-Ph groups appear around $3050\ \text{cm}^{-1}$. Peaks at 2970 and $2900\ \text{cm}^{-1}$ refer to the existence of Si-Me bonds. A strong absorption band due to the aliphatic C-H chain of PDLA-1,6-hexanediol was also detected at 2950

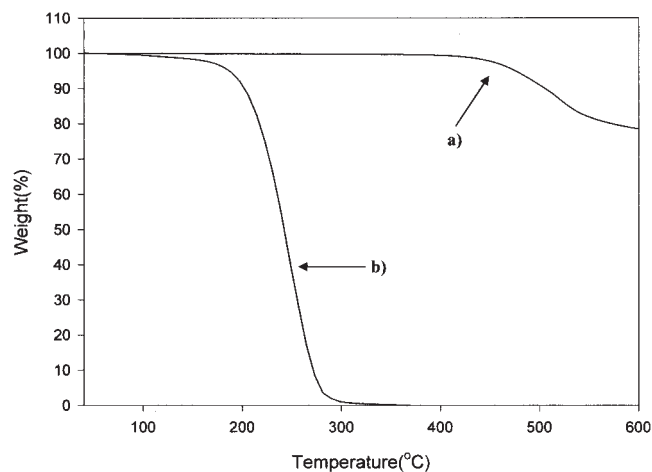


Figure 1 TGA thermograms of (a) uncured PMPSQ and (b) PDLA-1,6-hexanediol.

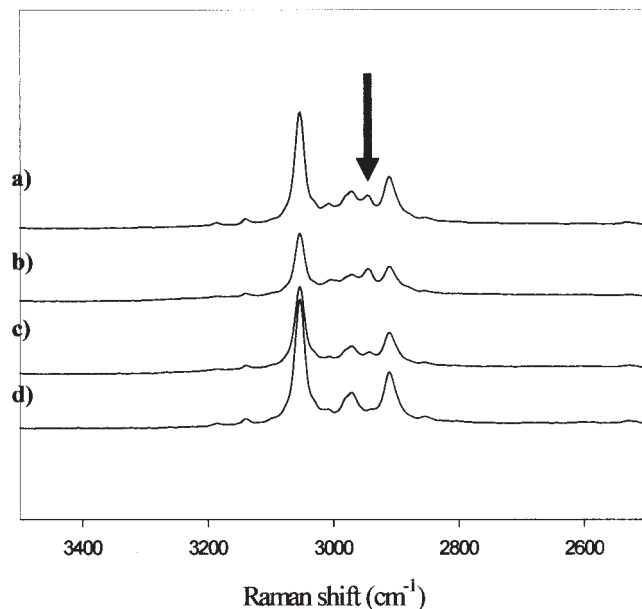


Figure 2 FT-Raman spectra of PMPSQ/PDLLA-1,6-hexanediol (80/20) hybrids (a) before foaming and after heating, (b) at 150°C for 2 h, (c) at 230°C for 3 h, and (d) at 300°C for 30 min.

cm^{-1} (see the arrow in Fig. 2). As temperature increases from 150 to 230°C, the peaks assigned for PDLLA-1,6-hexanediol became smaller [see Figs. 2(b–c)]. After the 3rd step (heating at 300°C for 30 min.) of the foaming process, characteristic peaks of PMPSQ were only detected as shown in Figure 2(d). Consequently, based on these results shown in Figures 1 and 2, the foaming condition was determined as shown in Figure 3. As a summary, the 1st step is to induce complete evaporation of residual solvent and initiate thermal decomposition of the porogen. Continuing pyrolysis of the porogen and a curing process of some defect structures of PMPSQ can be

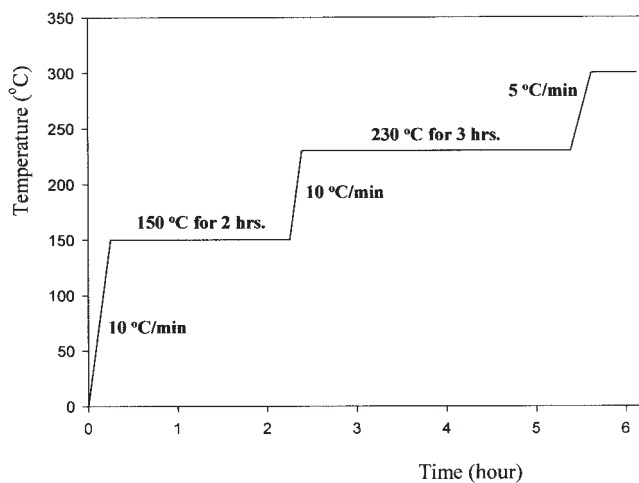


Figure 3 Optimized 3-step foaming condition.

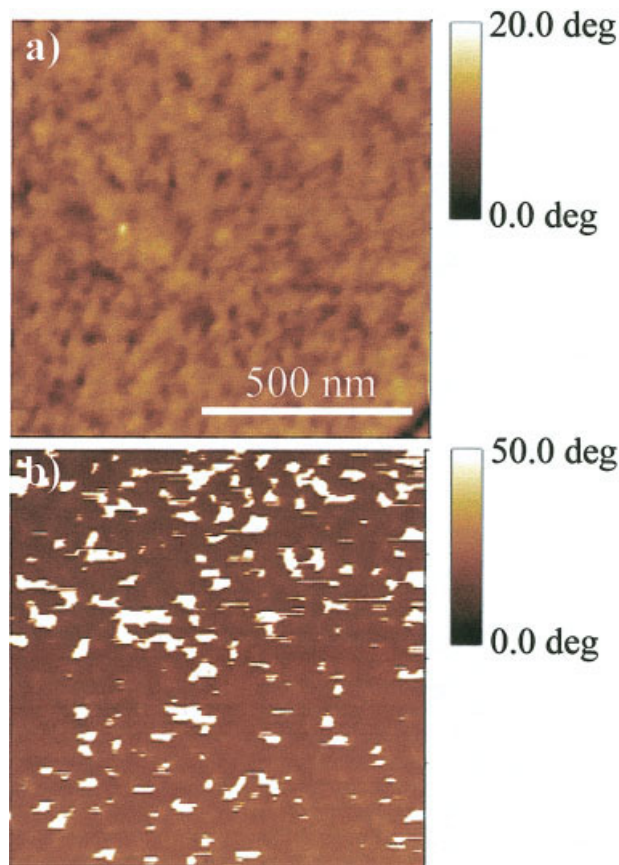


Figure 4 AFM phase images of PMPSQ/PDLLA-1,6-hexanediol (90/10) hybrid (a) before and (b) after foaming process. [Color figure can be viewed in the online issue, which is available at www.interscience.wiley.com.]

achieved at the 2nd step. The 3rd step results in complete pyrolysis of the thermally labile block and annealing of the matrix. On the basis of these results, the PMPSQ nanofoams were prepared according to the conditions described earlier.

Surface morphology of the nanofoamed PMPSQ thin films

Surface morphology of nanofoamed PMPSQ thin films were investigated by AFM as shown in Figures 4 and 5. AFM images of the nanofoamed films appear to have a different trend than our earlier results with inorganic/organic hybrids based on PSSQ and hydroxyl-functionalized polystyrene.^{19,24} The organic phase can be observed by tapping mode AFM due to the different surface tension of the polymer from the inorganic matrix (PMPSQ). The organic phase after nanofoaming appears as white spots in the phase images. These white spots likely resulted from the absence of interacting atomic force between the AFM tip and empty space (the foam phase). It can also be explained by the location of the foams. Since the foams are located just under the film surface, the foams will

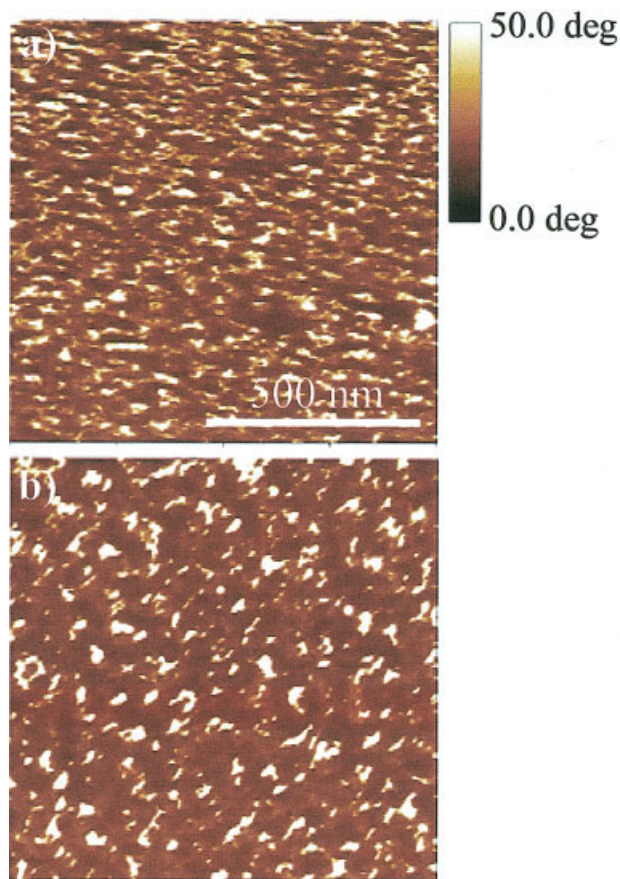


Figure 5 AFM phase images of nanofoamed PMPSQ films obtained from PMPSQ/PDLLA-1,6-hexanediol hybrids with composition of (a) 85/15 and (b) 80/20. [Color figure can be viewed in the online issue, which is available at www.interscience.wiley.com.]

be observed as bumps on the surface. In conjunction with other results, this evidence indicates that the foaming process was carried out appropriately.

For clear comparison between the organic phase and the foam phase, AFM images of PMPSQ/PDLLA-1,6-hexanediol hybrids were taken before and after the foaming process (Fig. 4). The number and domain size of the air foam phase increase with the increase in PDLLA-1,6-hexanediol content in the hybrids. As shown in Figure 4(b), AFM images of the nanofoamed PMPSQ obtained from the PMPSQ/PDLLA-1,6-hexanediol (90/10) hybrid reveal that the air foam phase is relatively irregular and the domain size varies in the range of 20–50 nm. This irregularity is probably due to undesired phase separation during hybridization of PMPSQ and PDLLA-1,6-hexanediol, meaning the PMPSQ matrix forms intrahydroxyl interactions rather than interhydroxyl interactions with PDLLA-1,6-hexanediol, preventing uniform and regular penetration of the porogen into the matrix.

The number of hydroxyl groups in PDLLA-1,6-hexanediol increases as the PDLLA-1,6-hexanediol con-

tent is increased (Fig. 5). The increased number of hydroxyl groups results in interaction between the two polymers. If the porogen content becomes higher than 20%, however, self-aggregation results in a co-continuous phase between the two polymers. Yang et al.¹³ also reported on the interconnectivity of the pores depending on the porogen loading and a percolation threshold of 20–25% of the mass fraction of the template by positronium annihilation lifetime spectroscopy. The AFM data show small, uniformly distributed foams prepared from the PMPSQ/PDLLA-1,6-hexanediol (85/15) hybrid. This uniform distribution suggests that the maximum degree of interaction between organic and inorganic polymers exists at the optimized component ratio. Our results suggest that a nanofoamed PMPSQ film with uniformly dispersed and small organic domains can be obtained at this optimized organic/inorganic component ratio.

Yoon²⁵ also reported on the preparation of low *K* materials. He suggested that nanofoamed low *K* materials without any deterioration of mechanical properties can be obtained if the size of air foams is below 5 nm. The nanofoamed PMPSQ described in this article have a relatively small pore size (10–30 nm). Thus, we can expect that the deterioration of good mechanical properties of PMPSQ would be minimized. We are currently preparing a report on the mechanical properties and suitability test for microelectronic devices of the nanofoamed PMPSQ.

Measurement of dielectric properties of the nanofoamed PMPSQ films

Dielectric constants of the nanofoamed PMPSQ samples over the range from 30 to 100°C are shown in Figure 6(a). All the measured materials exhibit temperature-dependent dielectric behaviors. The dielectric constant, ϵ' , was calculated from the capacitance according to

$$\epsilon' = \frac{cl}{\epsilon_0 A} \quad (1)$$

where ϵ_0 is the dielectric constant of vacuum state, $8.854 \times 10^{-12} \text{ F/m}$, c is the capacitance of thin films, l is film thickness, and A is the area of the Al electrode. The dielectric constants of the samples at 60°C at 1 MHz are 2.78, 2.53, 2.45, and 2.41. Theoretical and experimental values of dielectric constants with various air foam contents are shown in Figure 6(b). In Figure 6(b), the solid and dotted lines represent experimental dielectric results, together with the prediction of the dielectric constant from Maxwell-Garnett theory (MGT),²⁶ respectively. The experimental trend is in relatively good agreement with the simple theoretical estimates by MGT. The small discrepancies between experimental results and MGT prediction may be due

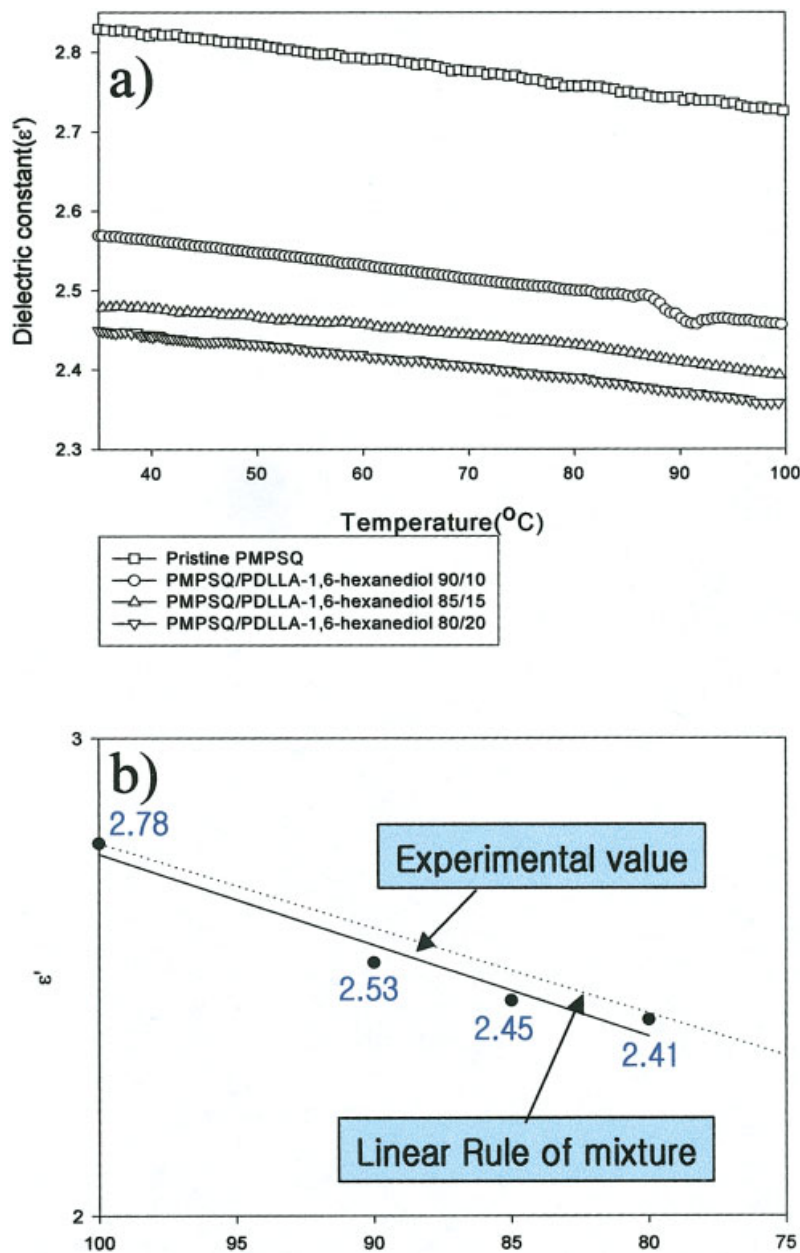


Figure 6 (a) Dielectric constants for the prepared PMPSQ nanofoams with temperature and (b) comparison of the estimated dielectric constants to the calculated values by Maxwell–Garnett theory. [Color figure can be viewed in the online issue, which is available at www.interscience.wiley.com.]

to an error in estimated porosities. The porosities were calculated from the weight fraction of the pore-forming thermally labile polymer (PDLLA-1,6-hexanediol) and that of the matrix material, assuming that the entire amount of PDLLA-1,6-hexanediol was involved in the phase separation. Exact values of actual porosity would result in closer agreement of dielectric constants dielectric constant measured and predicted. Nonetheless, values as low as 2.41 were measured.

CONCLUSIONS

To obtain nanofoamed PMPSQ with low dielectric constants, optimization of the foaming process should

be conducted prior to the industrial application of the PMPSQ nanofoaming process. Presented in this article are nanofoamed PMPSQ films with dielectric constant as low as 2.41. In the case of the hybrid containing a high content of porogen material (>20 wt %), however, enlarged pore size would be disadvantageous for industrial application of microelectronic packaging. Further foaming to obtain practically applicable nanofoamed PMPSQ with lower dielectric constants (below 2.0) cannot be carried out because an increase in porogen material leads to an increase in pore size. Larger pore size results in films with undesirable mechanical properties. Thus, we conclude that nano-

foamed PMPSQ with 15 wt % porogen material would be optimum. Nanofoamed PMPSQ with uniformly dispersed small air foam (below 5 nm) would be obtained if organic porogen and inorganic matrix are chemically bonded. Results regarding chemical bonding between the two polymers will be published in the future.

The authors thank Dr. Hyung-Jun Kim for his kind assistance with AFM measurement. Thanks are also extended to Dr. Dong Young Kim for his advice on FT-Raman experiments.

References

1. Maier, G. *Prog Polym Sci* 2001, 26, 3.
2. Hendricks, N. H. *Solid State Technol* 1995, 7, 117.
3. Sroog, C. E. *Prog Polym Sci* 1991, 16, 561.
4. Hedrick, J. L. *Macromolecules* 1991, 24, 6361.
5. Hedrick, J. L.; Hilborn, J. G.; Palmer, T.; Labadie, J. W.; Volksen, W. *J Polym Sci Part A: Polym Chem* 1990, 28, 2255.
6. Hedrick, J. L.; Labadie, J. W.; Volksen, W.; Hildorn, J. G. *Adv Polym Sci* 1999, 147, 61.
7. Kim, D. W.; Hwang, S. S.; Hong, S. M.; Yoo, H. O.; Hong, S. *Polymer* 2001, 42, 83.
8. Townsend, P. H.; Martin, S. J.; Godschalx, J.; Romer, D. R.; Smith, D. W.; Castillo, D., Jr.; DeVries, R.; Buske, G.; Rondan, N.; Froelicher, S.; Marshall, J.; Shaffer, E. O.; Im, J.-H. *Mater Res Soc Symp Proc* 1997, 476, 9.
9. Kirchhoff, R. A.; Bruza, K. *J Adv Polym Sci* 1994, 117, 1.
10. Case, C. B.; Case, C. J.; Kornblit, A.; Mills, M. E.; Castillo, D.; Liu, R. *Mater Res Soc Symp Proc* 1997, 443, 177.
11. Nguyen, C. V.; Carter, K. R.; Hawker, C. J.; Hedrick, J. L.; Jaffe, R. L.; Miller, R. D.; Remenar, J. F.; Rhee, H.-W.; Rice, P. M.; Toney, M. F.; Trollsas, M.; Yoon, D. Y. *Chem Mater* 1999, 11, 3080.
12. Baney, R. H.; Itoh, M.; Sakakibara, A.; Suzuki, T. *Chem Rev* 1995, 95, 1409.
13. Yang, S.; Mirau, P. A.; Pai, C.; Nalamasu, O.; Reichmanis, E.; Pai, J. C.; Obeng, Y. S.; Seputro, J.; Lin, E. K.; Lee, H.-J.; Sun, J.; Gidley, D. W. *Chem Mater* 2002, 14, 369.
14. Hwang, S. S.; Hong, S. M.; Lee, E. C.; Hong, S. *Jpn. Pat.* 13-149443 (2001).
15. Lee, E. C.; Kimura, Y. *Polym J* 1997, 29, 678.
16. Lee, E. C.; Kimura, Y. *Polym J* 1998, 30, 234.
17. Lee, E. C.; Kimura, Y. *Polym J* 1998, 30, 730.
18. Hong, S. MS Dissertation, Hanyang University, Seoul, Korea, 2001.
19. Hong, S.; Hong, S. M.; Hwang, S. S.; Kim, B. C. *J Appl Polym Sci* 2003, 90, 2801.
20. Hwang, T. G.; Hong, S.; Hwang, S. S.; Hong, S. M. Korea Institute of Science and Technology, unpublished work.
21. Lee, S. H. Ph.D. Dissertation, Hanyang University, Seoul, Korea, 2001.
22. Oh, W.; Hwang, Y.; Park, Y. H.; Ree, M.; Chu, S.-H.; Char, K.; Lee, K. J.; Kim, S. Y. *Polymer* 2003, 44, 2519.
23. Ma, J.; Shi, L.; Shi, Y.; Luo, S.; Xu, J. *J Appl Polym Sci* 2002, 85, 1077.
24. Kim, D. W.; Hwang, S. S.; Hong, S. M.; Lee, E. C. *Polym J* 2000, 32, 532.
25. Yoon, D. The Third International Symposium on Hyperstructured Organic Materials, Seoul National University, Seoul, Korea, 2001, Vol. 1.
26. Maxwell-Garnett, J. C. *Phil Trans R Soc* 1905, 205, 237.